New Electromigration Modeling and Analysis Considering Time-Varying Temperature and Current Densities

Hai-Bao Chen‡, Sheldon X.-D. Tan‡, Xin Huang‡ and Valeriy Sukharev §
‡ Department of Electrical Engineering, University of California, Riverside, CA 92521, USA
§ Mentor Graphics Corporation, Fremont, CA 94538, USA

Abstract—**Electromigration (EM) is projected to be the major reliability issue for current and future VLSI technologies. However, existing EM models and assessment techniques are mainly based on the constant current density and temperature. Such models will not work well at the system level as the current density (power) and temperature are changing with time due to different tasks (their loans) applied at run time. Existing EM approaches using average current density or temperature, however, will lead to significant errors as shown in this work. In this paper, we propose a new physics-based EM model considering time-varying temperature and current density, which reflects a more practical chip working conditions especially for multi-core and emerging 3D ICs. We study the impacts of the time-varying current densities and temperature profiles on EM-induced lifetime of a wire for both nucleation phase and growth phase. We propose a fast stress calculation method for given time-varying temperature and current densities for the nucleation phase. We further develop new formulae to compute the resistance changes in growth phase due to changing temperature and current densities. Experimental results show that the proposed method shows an excellent agreement with the detailed numerical analysis but with much improved efficiency.**

I. Introduction

Electromigration-induced reliability becomes a major design constraint in the current and future nanometer VLSI technologies. Continuous increase in the die size accompanying by reduction of metal wire sections and, hence by increase of the current densities, which is governed by technology scaling, results in an increasingly difficult EM signoff when the traditional EM checking approaches are employed.

The lifetime of EM failure mechanisms all have exponential relationships with temperature due to the Arrhenius model, which shows that the processor lifetime decreases exponentially with temperature [1]. Most chips go through EM signoff at a specific temperature, like 110°C or 115°C, which close to the maximum temperature allowed for a chip. However, at 100°C, there can be a huge degeneration; at 115°C, designers have to add 2X or 3X guard band to ensure the EM signoff [2]. Such conservative and overdesign will be no longer an option in current and future technologies because 3X guard band increase will significantly increase the buffer size and many other aspects of chips, which will lead to increasing currents, thus costs and powers of the chips.

Existing EM reliability assessment is mainly based on the semi-empirical Black's equation [3],

$$MTTF = Aj^{-n}exp\{E_a/kT\} \tag{1}$$

This work is supported in part by NSF grant under No. CCF-1255899, in part by Semiconductor Research Corporation(SRC) Grant under No. 2013-TJ-2417 and in part by Academic Senate COR Fellowship.

which calculates mean time-to-failure (MTTF) based on known current densities (j) and temperatures (T). Here, k is the Boltzmann's constant, E_a is the EM activation energy. The symbol A is a constant, which depends on a number of factors, including grain size, line structure and geometry, current density, thermal history, etc. Black has determined the value of n as equals to 2. However, it is a today's common understanding that n depends on residual stress and temperature [4], and its value is highly controversial and E_a is a function of the current density [4].

In addition, Black's equation, although quite simple, suffers following major problems in today's chip design. First, it only works for constant temperature and current density, which is not the case in the practical operations of the chip. Using the maximum temperature and current densities will lead to unnecessarily conservative and costly designs as mentioned earlier. If one can have a more accurate EM assessment considering the actual temperature profiles and power of a chip for running practical work loads, chip performance can be significantly improved, or the costs of chip can be reduced due to less aggressive guard bands used. Secondly Black's equation is an over-simplified model of the actual physics for EM failure mechanisms. It does not tell designers what happens before the MTTF and what options are available to maintain and improve the chip EM reliability before the chip fails, which is extremely important for system level reliability management. For high performance multi-core and emerging 3D microprocessors, dynamic reliability management has been merged to maximize system performance (or minimizing powers) under life time constraints [5]–[7]. However, existing EM model is difficult to use as it cannot tell the reliability impacts caused by the current densities in the previous time period the chip experiences. As a result, a dynamic EM model considering time-varying temperature and current densities is very desirable for system level reliability management.

A. Related works

Recently a more physics-based EM model and full-chip EM analysis technique have been proposed [8], [9] to mitigate some of those mentioned problems. The model is based on the approximate analytic solution of a dynamic hydrostatic stress diffusion equation considering many wires and material parameters. It explicitly models the EM failure development as two-phase process: the nucleation and growth phases. The EM model also allows the consideration of the impacts of existing residual stress as it models the EM induced failure as a stress development process. However, this physics-based

978-1-4799-7792-5/15/$31.00 ©2015 IEEE

model is still based on the MTTF for a constant temperature and current density.

Lu *et al.* studies the impacts of transient temperature and current density on the EM effects [10] and proposed a resource-like EM modeling method based on the EM-induced stress diffusion equation [11] and applied the model for dynamic reliability analysis later [12]. However, this model is still based on the Black's equation for MTTF prediction of each time period with constant temperature and current density. Its modeling of the impacts from changing current densities are less accurate as shown in this work. Further, It did not consider the dynamic EM modeling for the growth phase as this is ignored in the existing Black's equation.

In this paper, we propose a new physics-based *dynamic* EM model, to consider the impacts of transient temperature and current densities, which reflects a more practical chip working conditions especially for multi-core processors and emerging 3D ICs. It is based on the recently proposed more physics-based EM model [8], [9] with consideration of changing temperature and current densities. We study the impacts of the time-varying current densities and temperature profiles on EM-induced life time of a wire for both nucleation phase and growth phase. We propose a fast stress calculation method for given time-varying temperature and current densities for the nucleation phase. We further develop new formulae to compute the resistance changes of a wire in growth phase due to changing temperature and current densities. Experimental results show that the proposed method shows an excellent agreement with the detailed numerical analysis but much improved efficiency.

II. Analytic expressions for dynamic EM stress in nucleation phase

A. EM physics and the dynamic stress diffusion equation

In this section, we first present the basic dynamic stress diffusion equation along a metal line during electromigration, and then show the analytical solution for the stress during the void nucleation phase over time under typical boundary conditions. The proposed model will be validated against the finite element method based numerical analysis.

For a one dimensional metal wire, the stress $\sigma(t)$ developed in the metal wire due to EM effects is well described by the following dynamic stress diffusion-like equation [11] [13]:

$$\frac{\partial \sigma(x,t)}{\partial t} = \frac{\partial}{\partial x}[\kappa(\frac{\partial \sigma(x,t)}{\partial x} + G)], \tag{2}$$

where the diffusivity $\kappa = \frac{D_a B \Omega}{kT}$. κG and $\kappa \frac{\partial \sigma(x,t)}{\partial x}$ are the EM and back-stress induced fluxes. The D_a is is the effective diffusion coefficient obtained by averaging the diffusivities through grain boundaries, line interfaces, and grain interiors taken with geometrical waiting factors:

$$D_a = D_0 \exp(-\frac{E_a}{kT}), \tag{3}$$

where D_0 is the pre exponential factor. E_a is the activation energy, B is the applicable modulus, Ω is the atomic volume, k is Boltzmann's constant, T is the absolute temperature, E is the electric field, and q^* is the effective charge. The electric field E can be replaced by the product of the resistivity ρ times

TABLE I
Notations and typical value in our transient simulation

Term	Typical value	Description
ρ	1.67e-8Ω· m	Electrical resistivity
e	1.60e-19C	Electric charge
Z^*	10	Effective valence charge
Ω	8.78e-30 m^3	Atomic volume
k	1.38e-23J/K	Boltzmann constant
B	1e11Pa	Back flow stress modular
D_0	7.56e-5m^2/ s	Pre exponential factor of diffusion
E_a	0.8eV	Activation energy
σ_T	400MPa	Thermal stress
j	From simulation	Current density
T	From simulation	Absolute temperature
σ	From simulation	Electromigration stress

the current density j, i.e., $E = \rho j$. The effective charge $q^* = |Z^*|e$ is a known quantity, where e is the elementary charge and Z^* is the effective charge number. As a result, G can be re-written as $G = \frac{\rho j |Z^*| e}{\Omega}$. To facilitate the comprehension of this paper, we summarize the major notations in Table I.

Fig. 1 shows the stress development over time in a metal line computed by COMSOL [14], which is a finite element analysis tool. Over time, tensile (the positive) stress will be

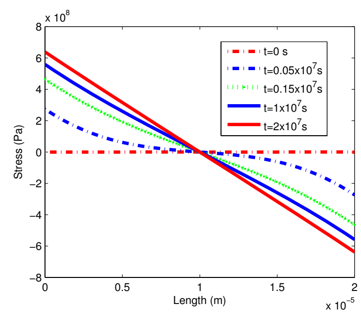

Fig. 1. The EM-induced stress development and distribution in a single metal wire

developed at the cathode node (left node) and compressive (negative) stress will be developed at the anode (right) node. The stress changes sign in the middle of the wire. The built-up stress (its gradient) will serve as the counter-force for atomic flux. If the largest stress at the cathode node exceeds critical stress (not shown in the figure), then voids will be created. If the stress development enter a steady state (atomic diffusion stops) before it reaches the critical stress, the wire will become immortal.

B. The analytic solution of the dynamic stress

Eq. (2) can have a closed-form solution under some boundary conditions. We first assume that the diffusivity κ is not the function of time. For the nucleation phase, the flux of stress is blocked at both ends $x = 0$ and $x = L$, i.e., $J(0,t) = J(L,t) = 0$ where $J(x,t) = \frac{D_a}{kT}(\frac{d\sigma(x,t)}{dx} + G)$.

The stress evolution in the line can be given as follows

$$\sigma(x,t,\kappa,G) = \sigma_T + GL\{\frac{1}{2} - \frac{x}{L} - 4\sum_{n=0}^{\infty} \frac{\cos((2n+1)\pi\frac{x}{L})}{(2n+1)^2\pi^2 \exp((2n+1)^2\pi^2\frac{\kappa t}{L^2})}\}, \tag{4}$$

where σ_T is the pre-existing residual stress due to a thermal process. In the existing EM modeling methods, where interest focuses on finding the nucleation time when the stress developed in the line has reached the critical stress [15]. To derive the closed-form expression, one can keep the slowest decaying term of the infinite series in (4) to obtain the approximate estimation for stress at the line cathode end ($x = 0$) as

$$\sigma(t, T, j) \approx \sigma_T + GL(\frac{1}{2} - \frac{1}{2\exp\{\frac{D_a B\Omega t}{L^2 kT}\}}). \quad (5)$$

As a result, when $\sigma(t, T, j) \geq \sigma_{crit}$, the nucleation time t_{nuc} can be computed in an analytic form as below [8], [9]

$$t_{nuc} = \frac{L^2 kT}{D_a B\Omega} \ln\{\frac{\frac{\rho j|Z^*|eL}{2\Omega}}{\sigma_T + \frac{\rho j|Z^*|eL}{2\Omega} - \sigma_{crit}}\}. \quad (6)$$

However, in our approach, we focus on the dynamic stress directly. As a result, we can use a more accurate analytic expression in (4) with sufficient number of terms.

III. The dynamic EM modeling in nucleation phase

In this section, we will present our new dynamic stress modeling and analysis technique to estimate electromigration lifetime under the time-varying temperature and current density environments.

A. Dynamic stress under time-varying temperature

We first describe the electromigration model to predict stress changes under time-varying temperature. We still start with the basic EM diffusion equation as shown in (2) . Now we re-write κ as

$$\kappa(T(t)) = \frac{D_0 \exp(-\frac{E_a}{kT(t)})B\Omega}{kT(t)}. \quad (7)$$

We assume that the current density doesn't change. Therefore, the term $G = \frac{Eq^*}{\Omega}$ is constant.

If we look at the complete analytic solution (4) (ignoring σ_T), only $\kappa(T(t))$ is affected by the temperature $T(t)$. As long as $\kappa(T(t))t$ is constant, stress $\sigma(T, t)$ will be the same. As a result, the temperature impact on the stress $\sigma(T, t)$ through $\kappa(T(t))$ can be translated to the time period change for a metal wire, which is also observed by [10]. In other words, a metal wire whose stress development over a period Δt_2 under temperature T_2 will be equal to stress development for a metal wire over a period $\frac{\kappa(T_2)}{\kappa(T_1)}\Delta T_2$ under temperature T_1. As a result, we convert the temperature-varying stress computation problem into the constant temperature problem again. Specifically, we assume that time period can be partitioned into n small segments:

$$\kappa(T(t)) = \begin{cases} \kappa_1, \ t \in [0, \ \Delta t_1], \\ \kappa_2, \ t \in (\Delta t_1, \ \Delta t_1 + \Delta t_2], \\ \cdots, \\ \kappa_i, \ t \in (\sum_{l=1}^{i-1} \Delta t_l, \ \sum_{l=1}^{i} \Delta t_l], \ i = 2, 3, \cdots. \end{cases} \quad (8)$$

Inside each time segment we assume that the temperature is constant. Now we denote the dynamic stress with time-varying temperature by $\sigma_{th}(x, t, \kappa, G)$. At the end of the first time segment $[0, \ \Delta t_1]$, we have $\sigma_{th}(x, \Delta t_1, \kappa_1, G) = \sigma(x, \Delta t_1, \kappa_1, G)$. Then at current time $t_i = \sum_{l=1}^{i} \Delta t_l$, we have

$$\sigma_{th}(x, \sum_{l=1}^{i} \Delta t_l, \kappa_i, G) = \sigma(x, \sum_{l=1}^{i} \frac{\kappa_l}{\kappa_1} \Delta t_l, \kappa_1, G), \quad (9)$$

where $i = 1, 2, \cdots$, and $\sigma(x, t, \kappa, G)$ is given by (4).

When the tensile stress (we ignore thermal residual σ_T for the time being for the sake of better presentation) reaches the critical stress σ_{crit}, a void will nucleate at the cathode end of a metal wire. If σ_{crit} is greater than the steady state tensile stress at the cathode end, no void will form and the wire is immortal. If the dynamic stress reaches a critical threshold at the i_{nuc}-th time segment, we have $\sigma_{crit} = \sigma(x, \sum_{l=1}^{i_{nuc}} \frac{\kappa_l}{\kappa_1} \Delta t_l, \kappa_1, G)$. Then the time to nucleation can be computed by $t_{nuc} = \sum_{l=1}^{i_{nuc}} \Delta t_l$.

B. Dynamic EM stress under time-varying current density

Now we study the EM stress development under changing current density over time with constant temperature. Different from the existing approaches, we show that taking average current density will not lead to the accurate solution for stress assessment in general.

Again, we look at the dynamic stress diffusion equation (2) in which the term $G = \frac{\rho j|Z^*|e}{\Omega}$ is a function of time. Now we assume that the temperature does not change over time, then the diffusion coefficient $\kappa = \frac{DB\Omega}{kT}$ is constant. In this case, however, there are no exact analytic solutions for the dynamic stress based on the time-varying current density.

Following the same technique as for the dynamic stress under time-varying temperature, we divide time into many segments such that the current density is constant within each time segment. In order to find the current stress in each time segment, the term $G(t)$ should be considered

$$G(t) = \begin{cases} G_1, \ t \in [0, \ \Delta t_1], \\ G_2, \ t \in (\Delta t_1, \ \Delta t_1 + \Delta t_2], \\ \cdots, \\ G_i, \ t \in (\sum_{l=1}^{i-1} \Delta t_l, \ \sum_{l=1}^{i} \Delta t_l], \ i = 2, 3, \cdots. \end{cases} \quad (10)$$

We denote the stress evolution with time-varying current densities by $\sigma_I(x, t, \kappa, G)$. At the end of the first time segment, the dynamic stress can be calculated by $\sigma_I(x, \Delta t_1, \kappa, G_1) = \sigma(x, \Delta t_1, \kappa, G_1)$ where $\sigma(x, t, \kappa, G)$ is given by (4). From (5), we observe that the term G determines the magnitude of the dynamic stress (while the temperature changes the frequency or changing rate of the dynamic stress in a sense). As a result, for each time segment, the only difference is the magnitude of the stress due to the time-varying current densities and the growth rates are the same. So if σ_I is accurate at $t_{i-1} = \sum_{l=1}^{i-1} \Delta t_l$, the dynamic stress at the current time $t_i = \sum_{l=1}^{i} \Delta t_l$

can be computed as

$$\sigma_I(x, \sum_{l=1}^{i} \Delta t_l, \kappa, G_i) = \sigma_I(x, \sum_{l=1}^{i-1} \Delta t_l, \kappa, G_{i-1}) + \sigma(x, \sum_{l=1}^{i} \Delta t_l, \kappa, G_i) - \sigma(x, \sum_{l=1}^{i-1} \Delta t_l, \kappa, G_i). \tag{11}$$

It can be verified that if there is no change for G_i, (11) gives the exact results compared to (4). In general, the accuracy and the computation time depend on the time step just as the general transient analysis.

C. Dynamic EM stress considering time-varying temperature and current density

Now we can handle the cases with both changing temperature and current densities as both are highly correlated in practice.

For the stress diffusion equation (2), now we have both diffusivity $\kappa(t) = \frac{D_a B \Omega}{kT(t)}$ and the term $G = \frac{\rho j |Z^*| e}{\Omega}$ changing over time. We follow the similar strategies we used in the previous cases: we divide time into multiple small segments. In each time segment, both the current and the temperature can be assumed to be constant. Without loss of generality, we assume that $\kappa(t)$ and $G(t)$ in each time segment Δt_i can be written as (8) and (10), respectively. At the end of the first time segment $[0, \Delta t_1]$, the combined dynamic stress $\sigma_{th,I}(x,t)$ can be given by $\sigma_{th,I}(x, \Delta t_1, \kappa_1, G_1) = \sigma(x, \Delta t_1, \kappa_1, G_1)$ where $\sigma(x, t, \kappa, G)$ is defined as (4). Combing the above-mentioned stresses $\sigma_{th}(x,t)$ and $\sigma_I(x,t)$, we can compute the combined dynamic stress at the end of the second time segment by $\sigma_{th,I}(x, \Delta t_1 + \Delta t_2, \kappa_2, G_2) = \sigma_{th,I}(x, \Delta t_1, \kappa_1, G_1) + \sigma(x, \Delta t_1 + \frac{\kappa_2}{\kappa_1}\Delta t_2, \kappa_1, G_2) - \sigma(x, \Delta t_1, \kappa_1, G_2)$. Based on the obtained stress $\sigma_{th,I}(x, \sum_{l=1}^{i-1} \Delta t_l, \kappa_{i-1}, G_{i-1})$ $(i \geq 3)$, then the dynamic stress at $t_i = \sum_{k=1}^{i} \Delta t_k$ can be computed as

$$\sigma_{th,I}(x, \sum_{l=1}^{i} \Delta t_l, \kappa_i, G_i) = \sigma_{th,I}(x, \sum_{l=1}^{i-1} \frac{\kappa_l}{\kappa_1} \Delta t_l, \kappa_{i-1}, G_{i-1}) + \sigma(x, \sum_{l=1}^{i} \frac{\kappa_l}{\kappa_1} \Delta t_l, \kappa_1, G_i) - \sigma(x, \sum_{l=1}^{i-1} \frac{\kappa_l}{\kappa_1} \Delta t_l, \kappa_1, G_i). \tag{12}$$

It can be verified that (12) is the general case for (9) and (11).

We now rewrite the formula (12) in a more compact integral form. Let us define

$$\beta(t) = L\{\frac{1}{2} - \frac{x}{L} - 4\sum_{n=0}^{\infty} \frac{\cos((2n+1)\pi \frac{x}{L})}{(2n+1)^2 \pi^2 \exp((2n+1)^2 \pi^2 \frac{\kappa(T(t))t}{L^2})}\}.$$

This allows for $\sigma(x, t, \kappa, G)$ in (4) to be rewritten as $\sigma(t) = \sigma_T + G(j)\beta(t)$. Let $t_i = \sum_{l=1}^{i} \Delta t_l$, (12) can be re-written as

$$\sigma(t) = \sigma(t_0) + \sum_{l=1}^{i} G_l \frac{\beta(t_l) - \beta(t_{l-1})}{\Delta t_l} \Delta t_l.$$

As $\Delta t_l \rightarrow dt$ and $G_l \rightarrow G(j(t))$, we derive the integral version for the proposed dynamic stress model

$$\sigma(t) = \sigma(t_0) + \int_{t_0}^{t} G(t)\beta'(t)dt. \tag{13}$$

Note that the $\beta(t)$ changing with time t can also come from time-varying temperature change as shown in $\kappa(T(t))$. As a result, (13) is also correct for the changing temperature case shown in (9).

IV. The EM dynamic model for growth phase

In the growth phase, void will start to grow, which will lead to an increase of wire resistance over time. Since the drift velocity of the void edge relates to atomic flux as $\vartheta = \Omega j$ [16], we can express it as

$$\vartheta = \frac{D_a}{kT} e|Z^*|\rho j. \tag{14}$$

Then, with the constant current density j, the void volume can be computed as $V_{void}(t) = \vartheta(t - t_{nuc})HW$, where W is the line width, H is the copper thickness (height). If both temperature and current density are time-varying, then (14) will be computed as

$$V_{void}(t) = HW \int_{t_{nuc}}^{t} \frac{D_0 \exp(-\frac{E_a}{kT(t)}) e|Z^*|\rho}{kT(t)} j(t)dt. \tag{15}$$

As a result, the resistance change for a metal wire will be

$$\Delta r(t) = \vartheta(t - t_{nuc}) \left[\frac{\rho_{Ta}}{h_{Ta}(2H + W)} - \frac{\rho_{Cu}}{HW} \right] \approx \frac{V_{void}(t)}{h_{Ta}(2H + W)HW}. \tag{16}$$

Here ρ_{Ta} and ρ_{Cu} are the resistivity of the barrier material (Ta/TaN) and copper and h_{Ta} is the barrier layer thickness. The top surface of metal wire does not have barrier.

The void growth process illustrated in Fig. 2 involves atomic transport over the whole metal line. It keeps increasing until the growth phase stops, which happens when steady state is reached with no atomic flux in the metal wire. For this state, the void reaches the so-called *saturation volume* which can be defined as [8]

$$V_{ss} = (\frac{\sigma_T}{B} + \frac{e|Z^*|\rho L j(t_{ss})}{2B\Omega})LWH. \tag{17}$$

The time when the growth phase stop is called t_{ss} in the line of length L. t_{ss} can be found from the solution of the equation $V_{void}(t_{ss}) = V_{ss}$.

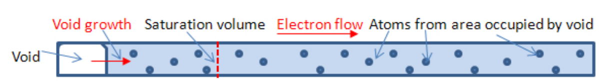

Fig. 2. The void growth process during the EM lifetime

Numerical methods can be used to obtain the approximate t_{ss} as there is not exact closed-form solution with the time-varying temperature and current density. Specifically, we define $f(\alpha, \beta) = \int_{\alpha}^{\beta} \frac{D_0 \exp(-\frac{E_a}{kT(t)}) e|Z^*|\rho}{kT(t)} j(t)dt$ for any pair of constants α and β, and $g(t) = (\frac{\sigma_T}{B} + \frac{e|Z^*|\rho L j(t)}{2B\Omega})L$ for any time t. By replacing integration with summation, we can estimate t_{ss} by the following algorithm:

1. Step1. Start: Choose a time-step size Δt and a given precision ε, and set $t_0 = t_{nuc}$.

2. Step2. Form the iteration: Set $i = 1$, and compute $f(t_{i-1}, t_i)$, $g(t_i)$, and $f(t_0, t_i) = f(t_0, t_{i-1}) + f(t_{i-1}, t_i)$ where $f(t_0, t_0) = 0$ and $t_i = t_{i-1} + \Delta t$.
3. Step3. If $| f(t_0, t_i) - g(t_i) | < \varepsilon$, set $t_{ss} = t_i$, else set $i = i + 1$, and go to Step2.

It should be pointed out that the computation of $f(\alpha, \beta)$ in the above algorithm can be simplified if both the temperature and the current density can be described as periodic pulsed waveforms, which can be seen as a good approximation for practical power/temperature traces in the practical situations. To model the effects of the periodic pulsed temperature and current density changes, we assume that the functions $T(t)$ and $j(t)$ have the following forms

$$T(t) = \begin{cases} T_1, \ t_{nuc} + mP \le t < t_{nuc} + (m + \frac{r}{2})P, \\ T_2, \ t_{nuc} + (m + \frac{r}{2})P \le t < t_{nuc} + (m+1)P, \end{cases}$$

$$j(t) = \begin{cases} j_1, \ t_{nuc} + mP \le t < t_{nuc} + (m + \frac{r}{2})P, \\ j_2, \ t_{nuc} + (m + \frac{r}{2})P \le t < t_{nuc} + (m+1)P, \end{cases}$$

where $m = 0, 1, 2, \cdots$, P is the period, and r is the duty ratio. In this case, the time t_{ss} can be calculated as a function of time $t_{ss} = t_{nuc} + KP$ where K satisfies the equation $f(t_{nuc}, t_{nuc} + KP) = g(t_{nuc} + KP)$.

V. Experimental results and discussions

The proposed dynamic EM model and analysis methods considering the varying impact of temperature and current density over time have been implemented in Matlab and tested on a single wire. In our numerical experiments, the material parameters used are shown in Table I and the total length of the wire is set to $20\mu m$.

The metal wire structure used in our experiment is shown in Fig. 3. In this figure, we also show a series of stress distributions on the wire at different times for this structure simulated in COMSOL [14]. The red color here presents the tensile stress while the blue color represents the compressive stress. As time goes by, more stress is built up at both ends of the wire until steady state is reached.

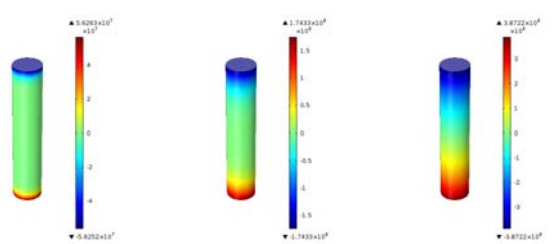

Fig. 3. EM stress distribution (Pa) at the instance in time: (a) $t = 2 \times 10^5$s; (b) $t = 2 \times 10^6$s; (c) $t = 1 \times 10^7$s.

We then study the dynamic stress considering the time-varying temperature and current densities. We create the periodic change temperature and current densities profiles, which are shown in Fig. 4(a) and Fig. 4(b), respectively.

We first study the new EM model with time-varying temperature and constant current. The varying temperature profiles over time are shown in Fig. 4(a). We apply the COMSOL [14] to compute an accurate numerical solution of (2). The results are shown in Fig. 5(a). From this figure, we can see that the stresses of the new model are in good agreement with those obtained from COMSOL. Fig. 5(a) also shows that if we take an average temperature during the total simulation time, there is a significant discrepancy between the stress developments obtained from the average temperature model and COMSOL.

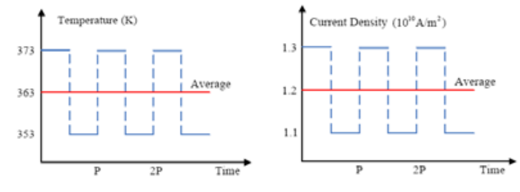

Fig. 4. (a) The temperature profiles during the EM lifetime. (b) The current density profiles during the EM lifetime.

Then we study the dynamic stress model under changing current densities and constant temperature. Fig. 5(b) shows the EM stress development over time at the cathode node of the wire with constant temperature and changing current densities as illustrated in Fig. 4(b). As we can see, the proposed method matches the numerical results given by COMSOL very well. While, again if we use the average current density to perform the simulation, then the results can make a significant difference. This is an important observation, which is different than existing approaches such as [10], which claim that average current density can be used for EM prediction.

Finally, we show the results for changing temperature and current densities. Fig. 5(c) shows the comparison results of the proposed method against COMSOL and the results based on the average values for both temperature and current densities. Again, we can see the proposed method matches the numerical results very well.

Now we study the nucleation time under different temperature and current density for the proposed method and the one using the average values. To observe the time to nucleation between the proposed method and the average model, we assume that the critical tensile stress is 400 MPa for our simulation. The results are shown in Fig. 6. It can be seen that significant nucleation time difference due to the EM stress evolution can be observed between these two models. While the proposed model gives much accurate estimation compared to the numerical results.

Now, we study the growth models under varying temperature and current densities. For the simulation of void growth phase, we assume that the nucleation time t_{nuc} in (16) is $10^7 s$. Fig. 7 shows the relative increases of resistance for the average-valued model and the new dynamic EM method. As can be seen in Fig. 7, the rate of resistance increase over time after void nucleation in the average-valued model is much slower than in the proposed dynamic model. Existing EM approaches using average temperature or current density can be only used to make conservative predictions of the resistance increase associated with EM-induced void growth.

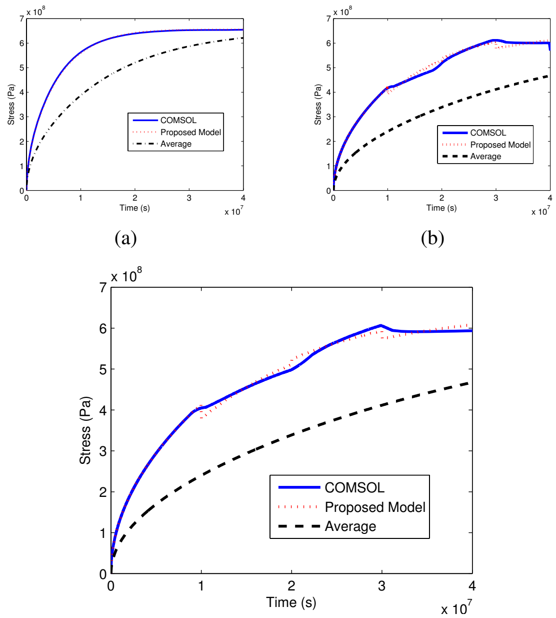

(a) (b)

(c)

Fig. 5. The EM stress development at the cathode node of the metal wire: (a) under changing temperature and constant current density; (b) under constant temperature and changing current density; (c) under time-varying temperature and current density.

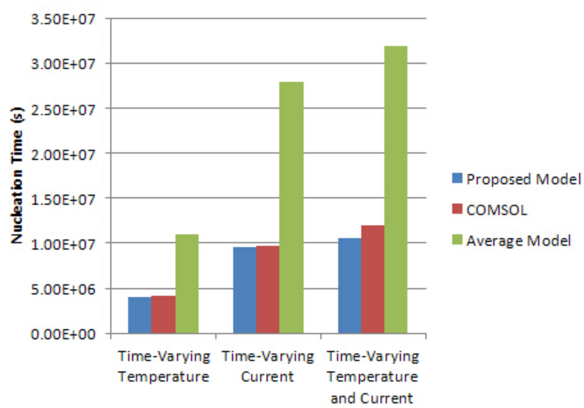

Fig. 6. Comparison of the nucleation time during the EM evolution.

VI. Conclusion

In this paper, we have proposed a new technique for physics-based EM analysis considering changing current density and temperature, which reflects a more practical chip working conditions especially for multi-core processors. We investigated the impacts of the time-varying current densities and temperature profiles on EM-induced lifetime of interconnect wires for both nucleation phase and growth phase. We developed a fast stress calculation method for given time-varying temperature and current densities for the nucleation phase. We further developed new formulae to compute the resistance changes of a wire in growth phase due to changing temperature and current densities. Experimental results have shown that the proposed method gives an excellent agreement with the detailed numerical analysis but with much improved efficiency.

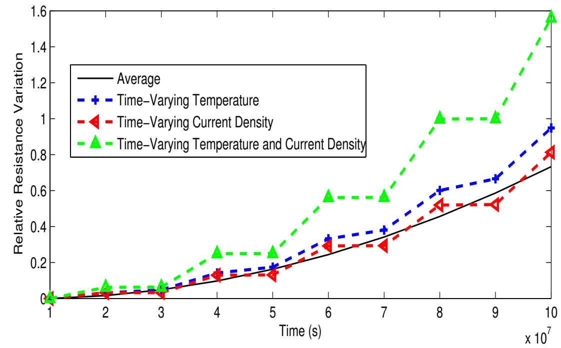

Fig. 7. Relative resistance variation with temperature and current density over time.

References

[1] "Failure Mechanisms and Models for Semiconductor Devices." In JEDEC Publication JEP122-A, Jedec Solid State Technolgy Association, 2002.
[2] B. Bailey, "Thermally challenged," in *Semiconductor Engineering*, 2013.
[3] J. R. Black, "Electromigration-A Brief Survey and Some Recent Results," *IEEE Transactions on Electron Devices*, vol. 16, no. 4, pp. 338–347, 1969.
[4] M. Hauschildt, C. Hennesthal, G. Talut, O. Aubel, M. Gall, K. B. Yeap, and E. Zschech, "Electromigration early failure void nucleation and growth phenomena in Cu and Cu(Mn) interconnects," in *2013 IEEE International Reliability Physics Symposium (IRPS)*, pp. 2C.1.1–2C.1.6, IEEE, 2013.
[5] J. Srinivasan, S. Adve, P. Bose, and J. Rivers, "Ramp: A model for reliability aware microprocessor design," *IBM Research Report*, 2003.
[6] T. Simunic, K. Mihic, and G. Micheli, *Optimization of Reliability and Power Consumption in Systems on a Chip*, vol. 3728 of *Lecture Notes in Computer Science*. Berlin, Heidelberg: Springer Berlin Heidelberg, 2005.
[7] E. Karl, D. Blaauw, D. Sylvester, and T. Mudge, "Reliability modeling and management in dynamic microprocessor-based systems," in *Design Automation Conference, 2006 43rd ACM/IEEE*, pp. 1057–1060, 2006.
[8] V. Sukharev, "Beyond black's equation full-chip em/sm assessness in 3d ic stack," *Microelectronic Engineering*, vol. 120, pp. 99–105, May 2014.
[9] X. Huang, T. Yu, V. Sukharev, and S. X.-D. Tan, "Physics-based electromigration assessment for power grid networks," in *Proc. Design Automation Conf. (DAC)*, June 2014.
[10] Z. Lu, W. Huang, J. Lach, M. Stan, and K. Skadron, "Interconnect lifetime prediction under dynamic stress for reliability-aware design," in *Proc. IEEE/ACM International Conferene on Computer-Aided Design (ICCAD)*, pp. 327–334, IEEE, Nov. 2004.
[11] M. A. Korhonen, P. Borgesen, K. N. Tu, and C. Y. Li, "Stress evolution due to electromigration in confined metal lines," *Journal of Applied Physics*, vol. 73, no. 8, pp. 3790–3799, 1993.
[12] Z. Lu, J. Lach, M. R. Stan, and K. Skadron, "Improved Thermal Management with Reliability Banking," *IEEE Micro*, vol. 25, no. 6, pp. 40–49, 2005.
[13] J. J. Clement, "Reliability analysis for encapsulated interconnect lines under dc and pulsed dc current using a continuum electromigration transport model," *Journal of Applied Physics*, vol. 82, no. 12, pp. 5991–6000, 1997.
[14] "Comsol multiphysics." http://www.comsol.com.
[15] J. J. Clement, S. P. Riege, R. Cvijetic, and C. V. Thompson, "Methodology for Electromigration Critical Threshold Design Rule Evaluation," *IEEE Trans. on Computer-aid Design of Integrated Circuits and Systems*, vol. 18, no. 5, pp. 576–581, 1999.
[16] Z. Suo, *Reliability of Interconnect Structures*, vol. 8 of *Comprehensive Structural Integrity*. Amsterdam: Elsevier, 2003.